

## Supplementary Information

# Arranging strategies for A-site cation: impact on stability and carrier migration of hybrid perovskite material

Wei Jian,<sup>a</sup> Ran Jia,<sup>a</sup> Hong-Xing Zhang,<sup>\*a</sup> and Fu-Quan Bai<sup>\*a,b</sup>

<sup>a</sup> *Laboratory of Theoretical and Computational Chemistry, Institute of Theoretical Chemistry and College of Chemistry, Jilin University, 130023, Changchun.*

<sup>b</sup> *Beijing National Laboratory for Molecular Sciences.*

*Email: baifq@jlu.edu.cn; zhanghx@jlu.edu.cn*

# Contents

<b>1</b>	<b>Computational Details</b>	<b>P1</b>
1.1	Calculation of tolerance factor . . . . .	P1
1.2	Crystal structure of $\text{FA}_{0.7}\text{MA}_{0.25}\text{Cs}_{0.05}\text{PbI}_3$ . . . . .	P1

## List of Tables

S1	Crystal structure and lattice parameters in this paper. . . . .	P3
S2	Variation in energy of valence band maxima (VBM), conduction band minima (CBM) and band gap at different temperature (eV). . . . .	P3

## List of Figures

S1	Calculated tolerance factors difference for FA/MA/Cs perovskites with different Cs ratios. . . . .	P4
S2	The optimized geometries, the valence band maxima (VBM) and conduction band minima (CBM) charge densities with different Cs ratios. Key: iodine, purple; hydrogen, white; carbon, cyan; nitrogen, brown; cesium, green. The electron density is shown in yellow and the value of isosurface is $2.5 \times 10^{-4} e \text{ \AA}^{-3}$ . . . . .	P5
S3	The relative ground state energy in $\text{FA}_{0.7}\text{MA}_{0.25}\text{Cs}_{0.05}\text{PbI}_3$ with different distributions of three cations. Two ordered simulation cells with lower ground-state energy at 0 K are shown. . . . .	P6
S4	The conduction band minima (CBM) charge densities of FAMACs-R and FAMACs-O. The electron density is shown in yellow and the value of isosurface is $1.5 \times 10^{-4} e \text{ \AA}^{-3}$ . . . . .	P7

S5	Dynamics of the inorganic framework in (a) FAMACs-R and (b) FAMACs-O. This plot represents the number density of atoms in space at 298 K. The ball-stick model of the inorganic framework shows the initial positions of Pb and I atoms. The scale is in arbitrary units, with blue and red indicating high and low number density, respectively. The yellow dashed circles highlight the positions of iodine atoms over the simulation. . . . .	P8
S6	Schematic structure of (a) FAMACs-R and (c) FAMACs-O at 298 K. The corresponding atomic displacements in (b) FAMACs-R and (d) FAMACs-O from MAPbI <sub>3</sub> to the optimized geometry at 298 K. . . . .	P9
S7	Density of states (DOS) of (a) FAMACs-R and (c) FAMACs-O at 298 K. Zero energy is set to the Fermi level. The valence band maxima (VBM) and conduction band minima (CBM) charge densities in the relaxed geometry of (b) FAMACs-R and (d) FAMACs-O. The electron density is shown in yellow and the value of isosurface is $1.5 \times 10^{-4} e \text{ \AA}^{-3}$ . . . . .	P10

# 1 Computational Details

## 1.1 Calculation of tolerance factor

For the perovskite structure, the commonly used and successful geometric ratio is the Goldschmidt tolerance factor,  $t$ . The success of predicting the perovskite structure by  $t$  in the  $\text{FAPbI}_3$  (0.987),  $\text{MAPbI}_3$  (0.912) and  $\text{CsPbI}_3$  (0.812) structures prompts us to extend the concept to mix-cations systems[1–3]. In this work, the atomic-ratio weighted average of FA, MA and Cs is utilized as the estimated effective cation size, defined as follows:

$$r_{effective} = 0.7r_{FA} + 0.25r_{MA} + 0.05r_{Cs} \quad (\text{S1})$$

$$t_{effective} = \frac{r_{effective} + r_{I^-}}{\sqrt{2}(r_{Pb^{2+}} + r_{I^-})} \quad (\text{S2})$$

where the ionic radius of  $r_{FA}$ ,  $r_{MA}$  and  $r_{Cs}$  are 2.53 Å, 2.17 Å and 1.69 Å, respectively.

## 1.2 Crystal structure of $\text{FA}_{0.7}\text{MA}_{0.25}\text{Cs}_{0.05}\text{PbI}_3$

The geometry and cell parameters for  $\text{FA}_{0.7}\text{MA}_{0.25}\text{Cs}_{0.05}\text{PbI}_3$  structures are fully optimized during the relaxation process. To probe the effect of the relative arrangements of cations in  $\text{FA}_{0.7}\text{MA}_{0.25}\text{Cs}_{0.05}\text{PbI}_3$ , various geometries with different ordering of FA, MA and Cs cations are built. The difference in ground-state energies among these systems is very large as shown in Figure S3. The right-side of Figure S3 indicates structures in which three cations are mixed as much as possible, while the left side is relatively ordered structures. It is noticed that there are two configurations with ordered arrangement of cations that are also stable (FAMACs-O2 and FAMACs-O3). However, in this work, we focus on the effects of ordered and random arrangements of  $\text{Cs}^+$  on the structure and performance of  $\text{FA}_{0.7}\text{MA}_{0.25}\text{Cs}_{0.05}\text{PbI}_3$ . Therefore, the lowest energy and most stable structure FAMACs-O is adopted to be the representative of the ordered arrangement for subsequent calculation.

**Table. S1** Crystal structure and lattice parameters in this paper.

Compound	Symmetry	Lattice constant (Å)	Band gap (eV)
CH <sub>3</sub> NH <sub>3</sub> PbI <sub>3</sub>	<i>Pm</i> $\bar{3}$ <i>m</i>	a = 6.29	1.66[4]
HC(NH <sub>2</sub> ) <sub>2</sub> PbI <sub>3</sub>	<i>Pm</i> $\bar{3}$ <i>m</i>	a = 6.36	1.47[5]
CsPbI <sub>3</sub>	<i>Pm</i> $\bar{3}$ <i>m</i>	a = 6.28	1.72[6]
FA <sub>0.7</sub> MA <sub>0.28</sub> Cs <sub>0.02</sub> PbI <sub>3</sub>		a = 6.35	1.37
FA <sub>0.7</sub> MA <sub>0.25</sub> Cs <sub>0.05</sub> PbI <sub>3</sub>		a = 6.33	1.56
FA <sub>0.7</sub> MA <sub>0.22</sub> Cs <sub>0.08</sub> PbI <sub>3</sub>		a = 6.32	1.40

**Table. S2** Variation in energy of valence band maxima (VBM), conduction band minima (CBM) and band gap at different temperature (eV).

Compound	VBM	CBM	Band gap
FAMACs-I (0 K)	-0.012	1.53	1.54
FAMACs-I (298 K)	-0.11	1.49	1.60
FAMACs-II (0 K)	-0.11	1.45	1.56
FAMACs-II (298 K)	-0.21	1.29	1.50

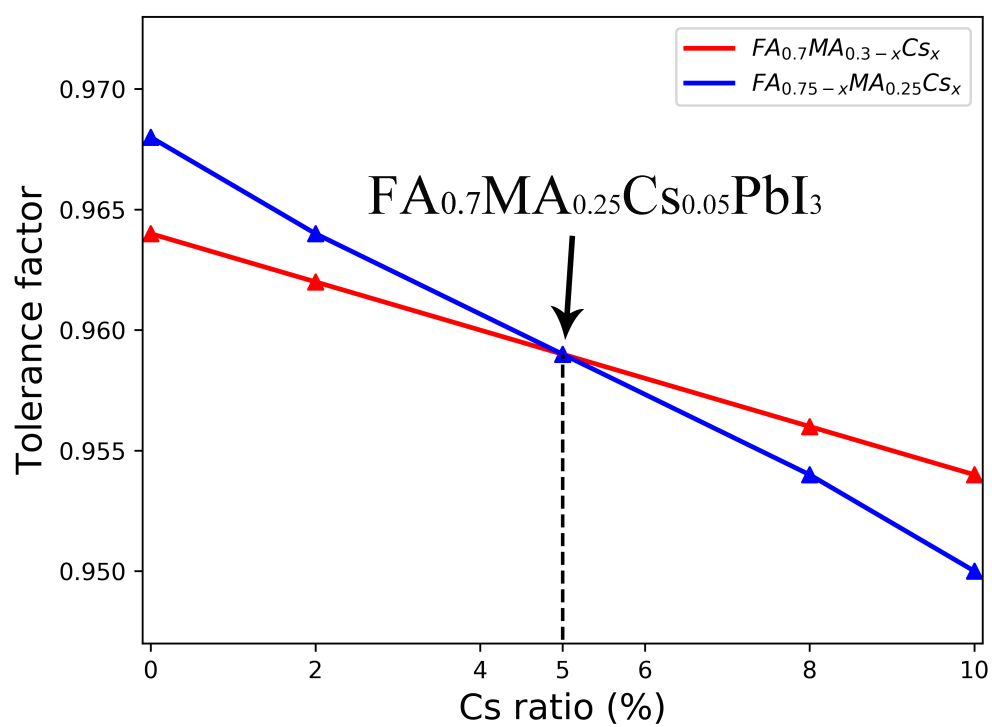


**Fig. S1** Calculated tolerance factors difference for FA/MA/Cs perovskites with different Cs ratios.

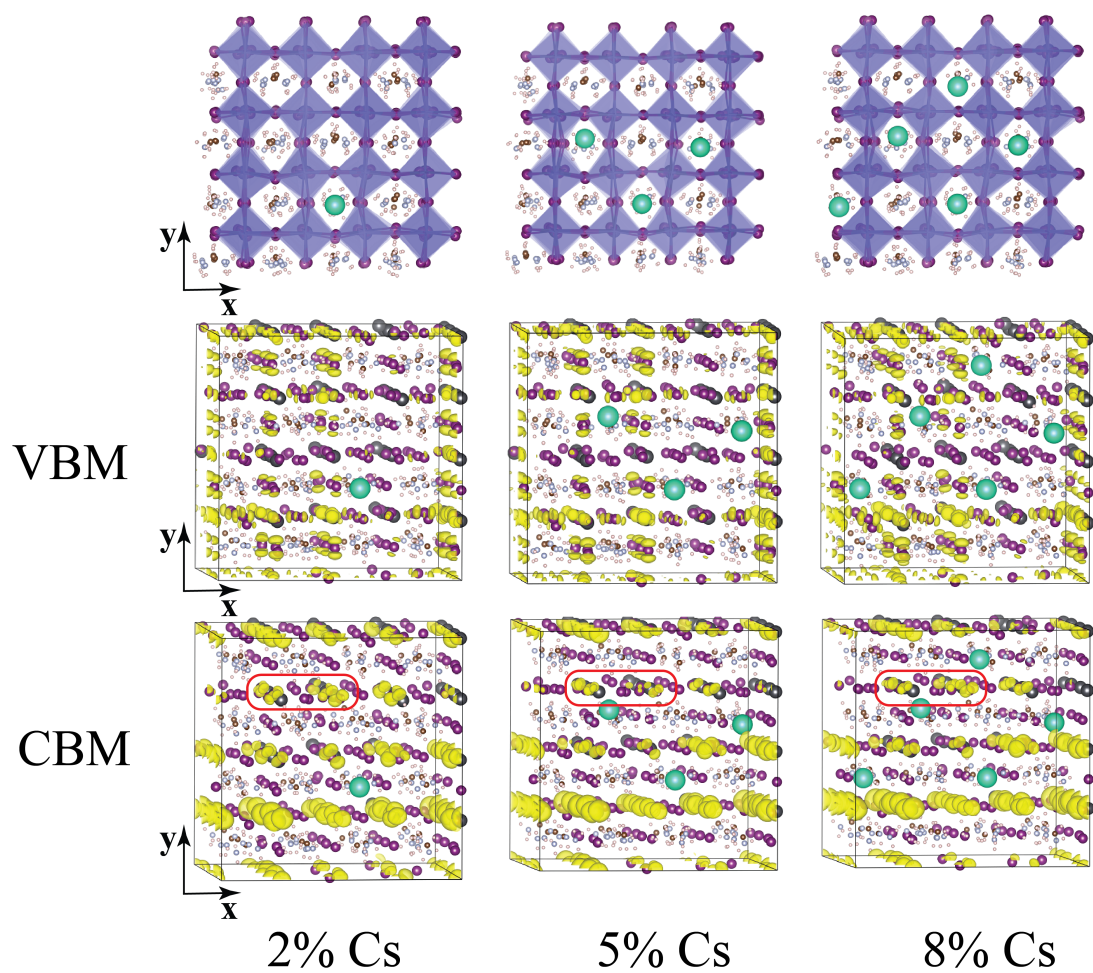


**Fig. S2** The optimized geometries, the valence band maxima (VBM) and conduction band minima (CBM) charge densities with different Cs ratios. Key: iodine, purple; hydrogen, white; carbon, cyan; nitrogen, brown; cesium, green. The electron density is shown in yellow and the value of isosurface is  $2.5 \times 10^{-4} e \text{ \AA}^{-3}$ .

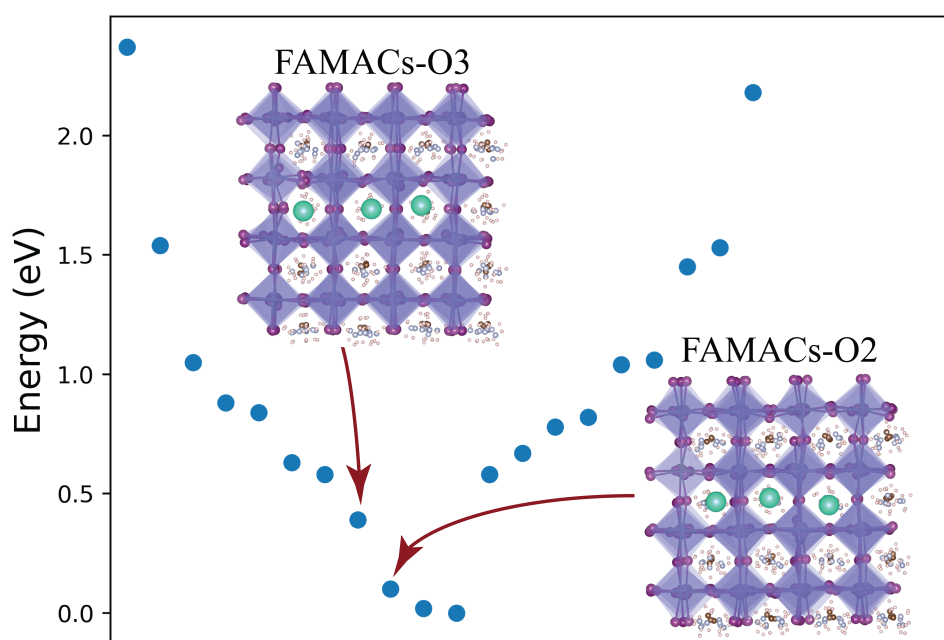


**Fig. S3** The relative ground state energy in  $\text{FA}_{0.7}\text{MA}_{0.25}\text{Cs}_{0.05}\text{PbI}_3$  with different distributions of three cations. Two ordered simulation cells with lower ground-state energy at 0 K are shown.



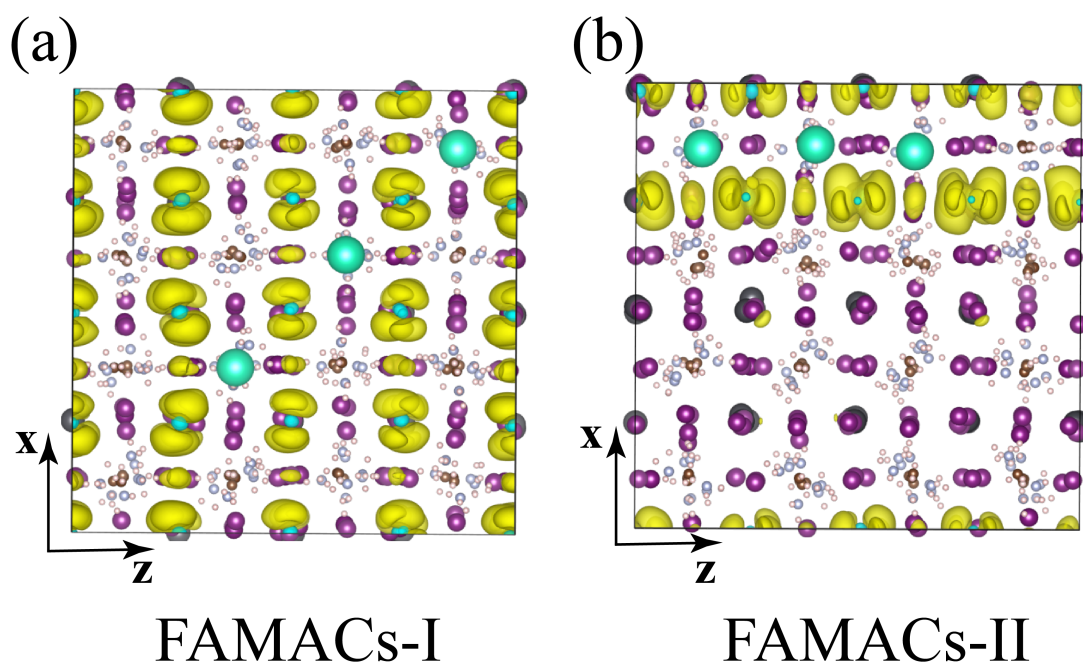


**Fig. S4** The conduction band minima (CBM) charge densities of FAMACs-R and FAMACs-O. The electron density is shown in yellow and the value of isosurface is  $1.5 \times 10^{-4} e \text{ \AA}^{-3}$ .

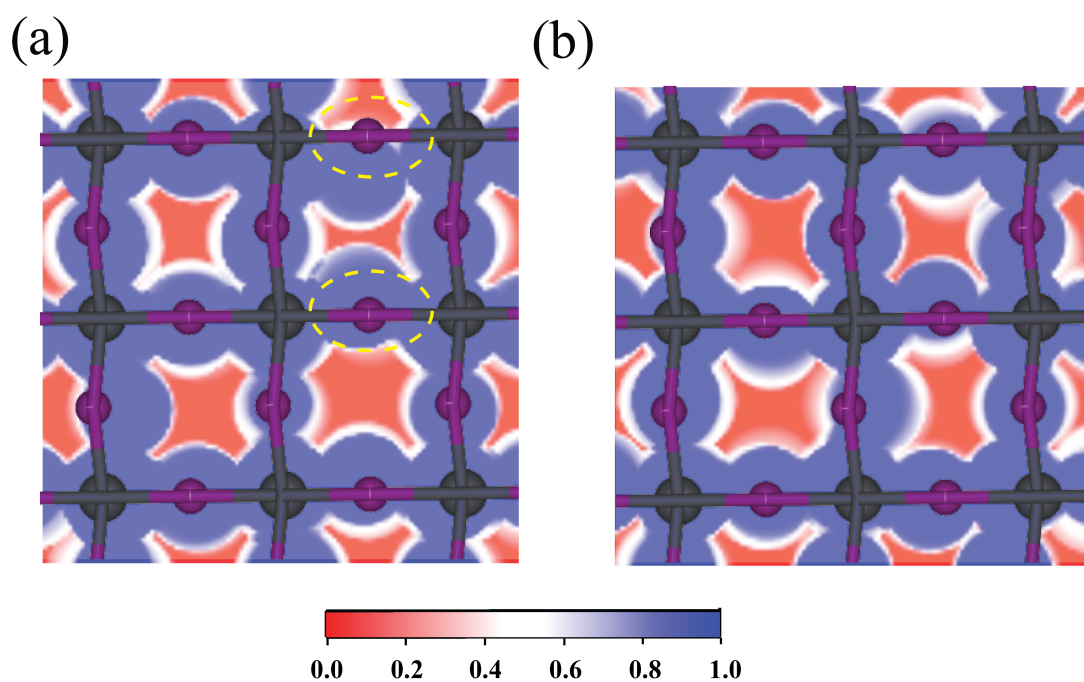


**Fig. S5** Dynamics of the inorganic framework in (a) FAMACs-R and (b) FAMACs-O. This plot represents the number density of atoms in space at 298 K. The ball-stick model of the inorganic framework shows the initial positions of Pb and I atoms. The scale is in arbitrary units, with blue and red indicating high and low number density, respectively. The yellow dashed circles highlight the positions of iodine atoms over the simulation.

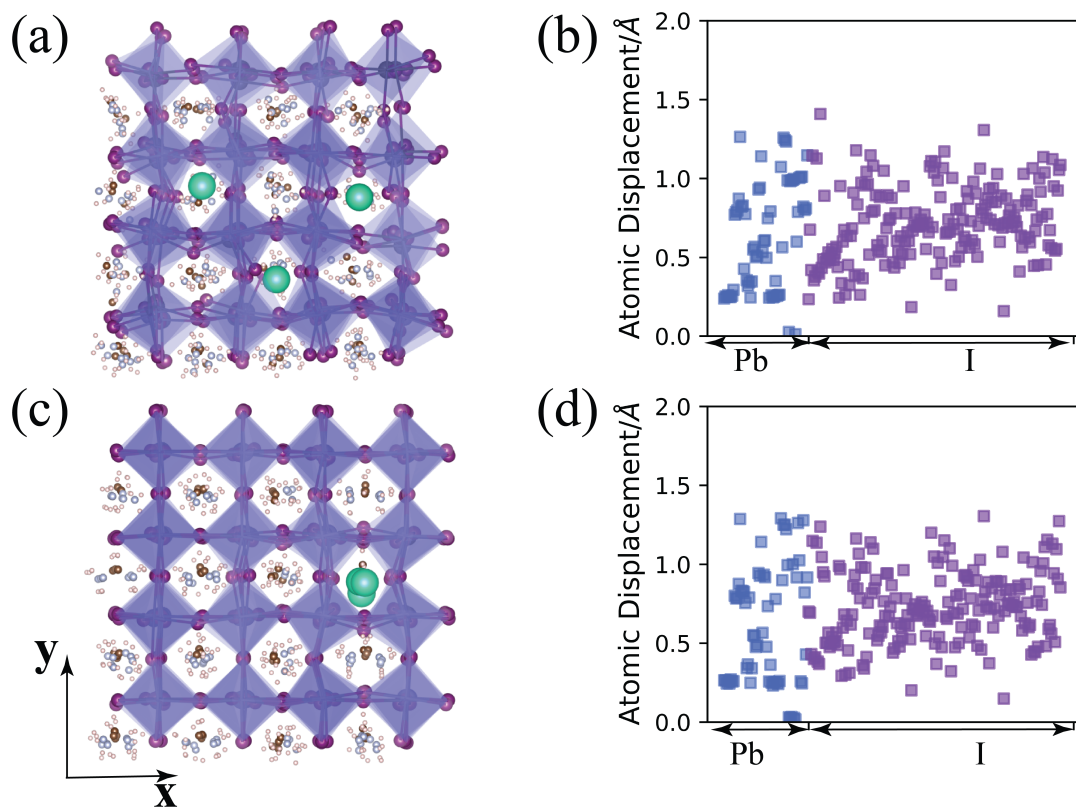


**Fig. S6** Schematic structure of (a) FAMACs-R and (c) FAMACs-O at 298 K. The corresponding atomic displacements in (b) FAMACs-R and (d) FAMACs-O from  $\text{MAPbI}_3$  to the optimized geometry at 298 K.

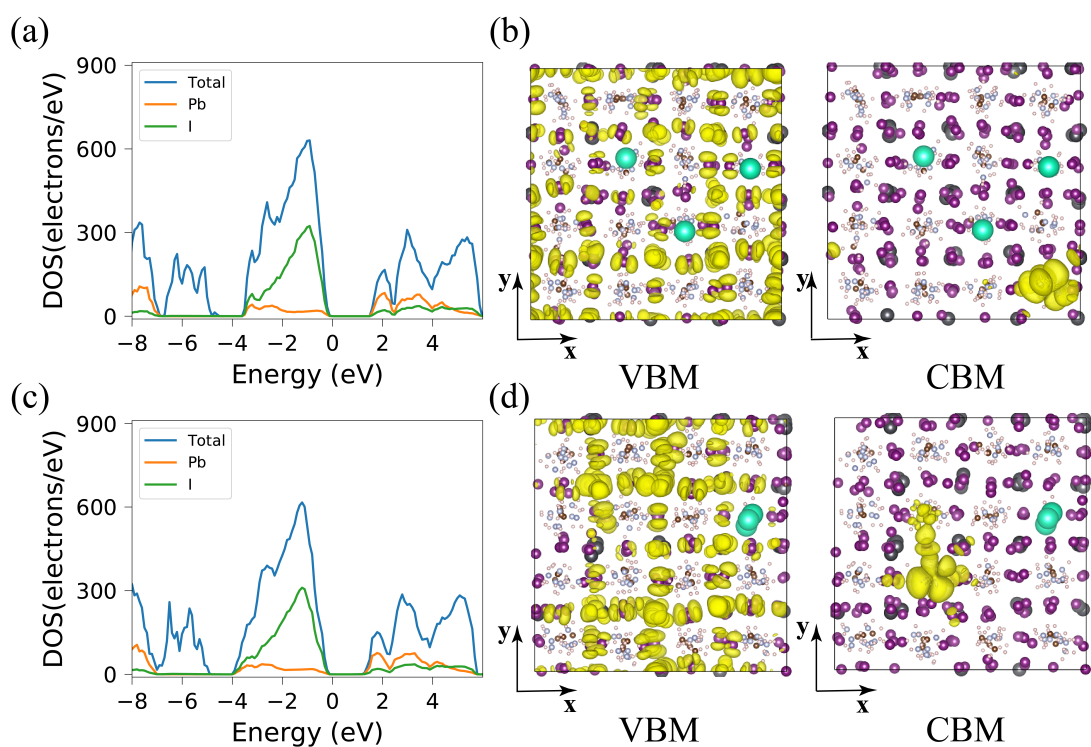


**Fig. S7** Density of states (DOS) of (a) FAMACs-R and (c) FAMACs-O at 298 K. Zero energy is set to the Fermi level. The valence band maxima (VBM) and conduction band minima (CBM) charge densities in the relaxed geometry of (b) FAMACs-R and (d) FAMACs-O. The electron density is shown in yellow and the value of isosurface is  $1.5 \times 10^{-4} e \text{ \AA}^{-3}$ .

## References

- [1] G. Kieslich, S. Sun and A. K. Cheetham, *Solid-state principles applied to organic–inorganic perovskites: new tricks for an old dog*, *Chemical Science*, 2014, **5**, 4712–4715.
- [2] W. Travis, E. Glover, H. Bronstein, D. Scanlon and R. Palgrave, *On the application of the tolerance factor to inorganic and hybrid halide perovskites: a revised system*, *Chemical science*, 2016, **7**, 4548–4556.
- [3] Z. Li, M. Yang, J.-S. Park, S.-H. Wei, J. J. Berry and K. Zhu, *Stabilizing perovskite structures by tuning tolerance factor: formation of formamidinium and cesium lead iodide solid-state alloys*, *Chemistry of Materials*, 2015, **28**, 284–292.
- [4] H. Tsai, R. Asadpour, J.-C. Blancon, C. C. Stoumpos, O. Durand, J. W. Strzalka, B. Chen, R. Verduzco, P. M. Ajayan, S. Tretiak *et al.*, *Light-induced lattice expansion leads to high-efficiency perovskite solar cells*, *Science*, 2018, **360**, 67–70.
- [5] M. T. Weller, O. J. Weber, J. M. Frost and A. Walsh, *Cubic perovskite structure of black formamidinium lead iodide,  $\alpha$ -[HC(NH<sub>2</sub>)<sub>2</sub>]PbI<sub>3</sub>, at 298 K*, *The journal of physical chemistry letters*, 2015, **6**, 3209–3212.
- [6] D. Trots and S. Myagkota, *High-temperature structural evolution of caesium and rubidium triiodoplumbates*, *Journal of Physics and Chemistry of Solids*, 2008, **69**, 2520–2526.